

Structure and properties of sintered tool gradient materials

L.A. Dobrzański, B. Dołżańska*

Institute of Engineering Materials and Biomaterials, Silesian University of Technology, ul. Konarskiego 18a, 44-100 Gliwice, Poland

* Corresponding author: E-mail address: barbara.dolzanska@polsl.pl

Abstract

Purpose: The main objective of the presented is to elaborate the fabrication technology of novel sintered tool gradient materials on the basis of hard wolfram carbide phase with cobalt binding phase, and to carry out research studies on the structure and properties of the newly elaborated sintered tool gradient materials.

Design/methodology/approach: The following research studies have been carried out to elaborate a new group of sintered tool gradient materials, wolfram carbide with cobalt matrix, to elaborate their fabrication technology and to determine their structure and properties: a fabrication technology of mixtures and the formation technology of wolfram carbide gradient materials with cobalt matrix WC-Co was applied and elaborated; sintering conditions were selected experimentally: time, temperature and sintering atmosphere as well as isostatic condensation, ensuring the best structure and properties; phase and chemical composition of the sintered gradient WC-Co materials was determined using EDX, EBSD methods and qualitative X-ray analysis; the structure of sintered gradient WC-Co materials was investigated using scanning microscopy and transmission electron microscopy; mechanical and physical properties of sintered gradient WC-Co materials was determined: porosity, density, hardness, resistance to abrasive wear, resistance to brittle cracking.

Findings: The presented research results confirm that the newly elaborated technology of powder metallurgy, which consists in sequential coating of the moulding with layers having the increasing content of carbides and decreasing concentration of cobalt, and then sintering such a compact, ensures the acquisition of the required structure and properties, including the resistance to cracking and abrasive wear of tool gradient materials, due to earned high hardness and resistance to abrasive wear on the surface as well as high resistance to cracking in the core of the materials fabricated in such a way.

Practical implications: *The material presented in this paper is characterized by very high hardness of the surface and relative ductility of the core. TGM with smooth changes of the cobalt phase in the material.*

Originality/value: *The obtained results show the possibility to manufacture TGMs on the basis of different portions of cobalt reinforced with hard ceramics particles in order to improve the abrasive resistance and ductility of tool cutting materials.*

Keywords: *Cemented carbides; Mechanical alloying; Powder Metallurgy*

Reference to this paper should be given in the following way:

L.A. Dobrzański, B. Dołżańska, Structure and properties of sintered tool gradient materials, in L.A. Dobrzański (ed.) Effect of casting, plastic forming or surface technologies on the structure and properties of the selected engineering materials, Open Access Library, Volume 1, 2011, pp. 89-132.

1. Introduction

A rapid development of the industry, technology and know-how induces the introduction of higher standards to meet the requirements which the cemented tool materials have to satisfy with respect to mechanical properties and resistance to wear. The functional properties of many products and of their components depend not only on the ability to transfer mechanical load through the whole active section of the component, on its physicochemical properties but also on the structure and properties of the material. The common fault of the operating tools is their tendency to crack, which in most cases eliminate the tool from further service, and the wear gradually and progressively diminishes its operating efficiency. Hence the resistance to cracking is a basic property, since the occurrence of minute microstructural defects results in the formation and propagation of cracks, whereas the resistance to wear stays unchanged [9,21, 39,49,58].

A considerable share of cobalt matrix results in high ductility of the core, since the propagation of a crack through cobalt is connected with the dissipation of relatively high energy. In contrast, transcrystalline cracks through carbide grains have the character of low energy brittle cracks. The combination of high hardness and resistance to abrasive wear with high resistance to brittle cracking is unobtainable in one homogeneous material. The acquisition of tool materials (Tool Gradient Materials (TGMs)) fabricated with the use of

powder metallurgy method, in effect of the gradient change of binding cobalt phase and the reinforcing phase of wolfram carbide, aims to solve the problem involving the combination of high hardness and resistance to abrasive wear with high resistance to brittle cracking, and consequently, to ensure their optimal synergy with operating conditions. The cutting edges of drill bits should combine in themselves these two contradictory properties where the surface layer is resistant to abrasive wear and the base is characterized by raised resistance to brittle cracking (Fig. 1) [1-10,17,23,33,60].



Figure 1. Diagram of the cemented tool gradient material [49]

One of numerous methods facilitating the fabrication of tool gradient materials is the technology of powder metallurgy. Through the application of the powder metallurgy technology for the fabrication of tool gradient materials we can closely control the chemical and phase composition as well as the structure of particular material layers [34-36,60]. In the Institute of Engineering Materials, at the Division of Materials Processing Technology, Management and Computer Techniques in Materials Science, research studies have been carried out for several years yielding the elaboration of a fabrication method of tool gradient materials with the application of powder metallurgy technology [23,34-49,50,53-56,59]. The desired material structure was obtained by the preparation of appropriate mixtures from the powder of wolfram carbide and cobalt, selection of suitable pressing pressure and technological conditions of cementing.

The objective of the presented here is to elaborate a fabrication technology of the newly developed cemented tool gradient materials on the basis of hard phase of wolfram carbide with the cobalt binding phase, and to carry out research studies on the structure and properties of the newly elaborated cemented tool gradient materials.

2. Experimental

2.1. Material and preparation of specimens for analysis

The analysis was carried out on specimens produced with the conventional method of powder metallurgy which consists in compacting in a closed moulding the successive, added layers having a gradually changing volumetric share of cobalt and wolfram carbide. In the research studies, we applied the powders of wolfram carbide (Fig. 2) and of cobalt (Fig. 3), having the chemical properties presented in Table 1. When selecting the material, we accepted the requirements involving its application in agreement with the Standard PN-ISO 513:1999.

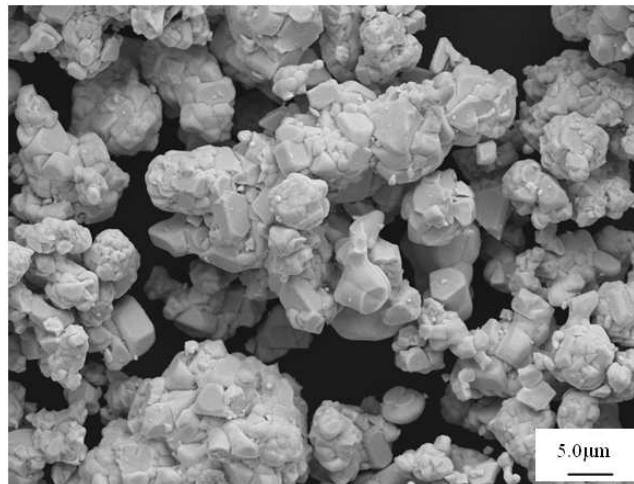


Figure 2. Wolfram carbide powder

The material for analysis was being prepared in two stages. In the first stage of the studies a set of mixtures of different chemical composition was elaborated, and then the compacts from wolfram carbide with cobalt matrix were formed, coating the moulding with successive layers of variable phase composition (Table 2). The selection of chemical composition of the materials was made experimentally through the change of cobalt concentration as the binding phase within the range from 3 to 15% and the share of wolfram carbide from 97 to 85%. The formation of the wolfram carbide and cobalt powder mixtures consisted in the preparation of appropriate portions of the said powders, adding each time paraffin as a sliding agent of the volumetric share of 2%. The powders prepared in this way were ground within the time

interval from 1 to 20 hours in a high-energy mill with ceramic balls (Fig. 4) and in a planetary ball mill with the balls from cemented carbides in order to make the powders homogeneous/uniform (Fig. 5). It was determined after the preliminary analyses that the time of 8 hours is long enough to ensure the homogeneity of the mixture and to coat the carbide grains with a cobalt layer.

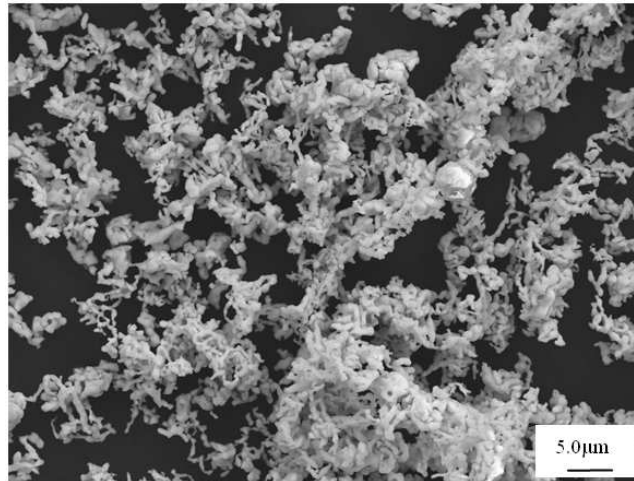


Figure 3. Cobalt powder

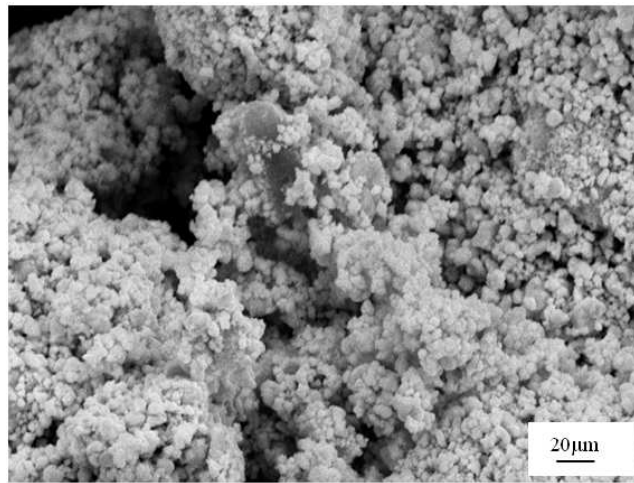


Figure 4. Mixture of WC powder (97%), Co powder (3%) after 8 hours of milling in the high-energy mill of the spex type

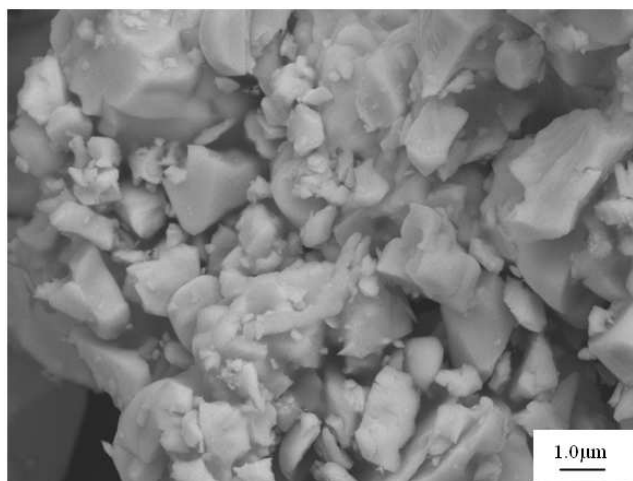


Figure 5. Mixture of WC powder (97%), Co powder (3%) after 8 hours of milling in the ball mill

Table 1. Chemical composition of powders from wolfram carbide and cobalt

Element	Mass concentration of particular elements in the powder	
	WC	Co
Mn	< 0.001	< 0.001
Ca	< 0.001	< 0.001
Zn	< 0.001	< 0.001
Si	< 0.002	< 0.002
Pb	< 0.002	< 0.002
Ni	< 0.002	< 0.002
S	< 0.002	< 0.002
Cu	< 0.002	< 0.002
O	0.45	0.45
Co	0.09	-
C	0.02	0.02

Using the obtained mixtures, WC-Co compacts were prepared for analysis in which, from the surface side of the layer, successive transit layers were formed with progressively lower share of wolfram carbide down to the base. The pressure during the pressing was being selected experimentally, pressing the powders in a closed moulding on a uniaxial hydraulic press under the pressure changing within the range from 300 to 450 MPa. The pressing

pressure was being selected by testing the densification of the powder mixture and observing the metallographic compacts. Ultimately, the pressure of 340 MPa was selected for further analyses.

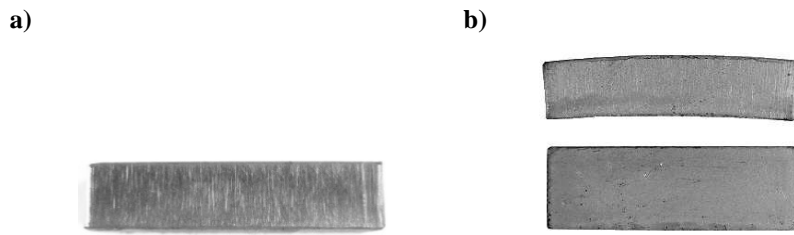


Figure 6. a) Compact pressed under the pressure of 340MPa from the 3-7%Co/97-73%WC_5 material, b) cemented tool material 3-7%Co/97-93%WC_5

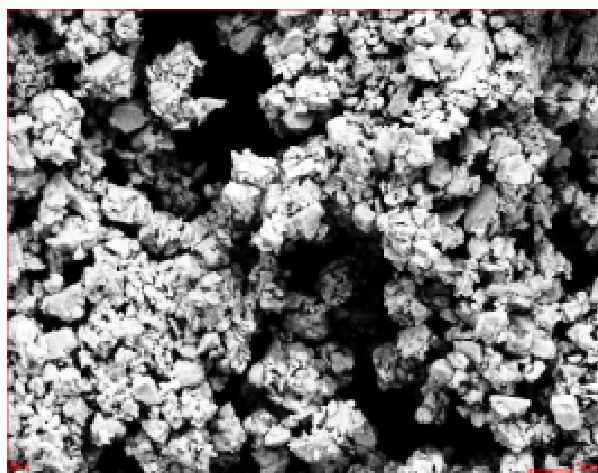
The compacts prepared in this way were characterized by smooth surface and had no signs of cracking, delamination or chipping (Fig. 6). The denotation of specimens and the volumetric share of the particular components in the mixture is presented in Table.2.

The cementing of the produced compacts was carried out in a vacuum furnace at the temperature $T_{sp}=1450^{\circ}\text{C}$ (Fig. 6b). Then, basing on the preliminary macroscopic observations of the sinters and on the porosity and density tests, assuming low porosity and high density as a selection criterion, a four-layer material containing from 3 to 9% of Co and from 97 to 91% of Co was selected for further research. During the selection process we were also taking into account the structure demonstrating uniform distribution of particular components in a given layer and the lack of surface deformation of the sinter. It was found, basing on preliminary metallographic observations and on the analyses of gradient porosity and density of tool materials having different number of layers and different phase composition of particular layers, that an excessive rise of the phase share difference between successive layers of the material has a negative influence on the structure and properties of the material.

Table 2. Denotation of WC-Co tool gradient material specimens

Denotation	3-15Co/97-85WC_3	3-9Co/97-91WC_4	3-7Co/97-93WC_5	3-15Co/97-85WC_5
Material type	3%Co+97% WC	3%Co+97% WC	3%Co+97% WC	3%Co+97% WC
	9%Co+91% WC	5%Co+95% WC	4%Co+96% WC	6%Co+94% WC
	15%Co+85% WC	7%Co+93% WC	5%Co+95% WC	9%Co+91% WC
		9%Co+91% WC	6%Co+94% WC	12%Co+88% WC
			7%Co+93% WC	15%Co+85% WC

a)



b)

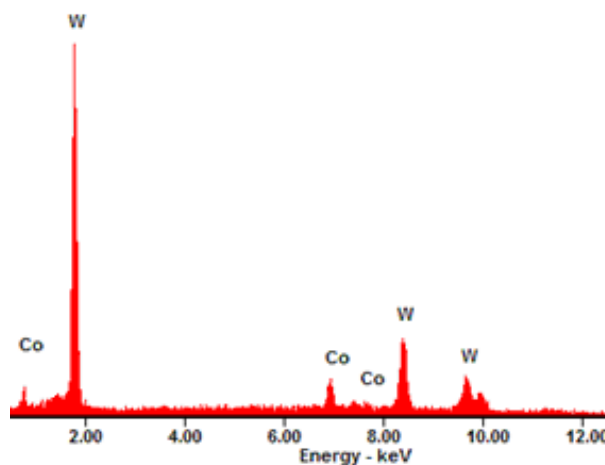


Figure 7. a) Mixture of WC powder (97%), Co powder (3%) after 8 hours of milling in a ball mill, b) Intensity graph as the function of the energy dispersion intensity of X-ray radiation for the WC powder (97%), Co powder (3%) after 8 hours of milling in a ball mill

The second stage of research involving the applied material fabrication technology consisted in milling the selected mixtures of wolfram carbide and cobalt in a ball mill with carbide balls for 8 hours (Fig. 7). The produced powder mixtures were then scattered down into the moulding, which yielded layers of gradually changing volumetric concentration of cobalt

and wolfram carbide share. In the material of the volumetric concentration of 3% Co and 97%WC in the surface layer, four further transit layers were formed with the 2% rise of cobalt concentration, down to the base layer containing 9% of Co and 91% of WC. Hence the denotation of the specimen being 3-9Co/97-91WC_4 (Table 2). The compacts were obtained in effect of the pressing at the already determined pressure of 340 MPa.

Then, basing on literature analysis [12-19, 28-32, 41-49, 53, 59], cementing conditions were selected experimentally. The specimens were cemented in a vacuum furnace in the conditions presented in the Table 3. In order to obtain better densification level, after the ultimate cementing, the condensation of sinters through hot isostatic pressing – HIP) was applied at the temperature of 1425°C and under the pressure of 200 MPa, as well as the sintering technology under pressure (Sinter-HIP) at the temperature of 1420°C and under the pressure of 6 MPa (Table 3).

Table 3. Cementing conditions for the newly elaborated tool gradient material 3-9%Co/97-91%WC

Cementing type	Cementing conditions	
	t _{sp} [min]	T _{sp}
Unbound	30	1400°C 1430°C 1460°C
With isostatic condensation	90	1400°C 1430°C 1460°C
Under pressure	60	1420°C

In one apparatus and in one cycle the processes of deparaffination, cementing and hot isostatic condensation in argon atmosphere under the pressure of 6 MPa were carried out. Then, for the obtained tool gradient materials, metallographic tests were carried out, physical and mechanical properties of the sinters were determined and the distribution of eigen-stresses in the material after sintering and during the operation were analyzed.

2.2. Methodology

The density of the cemented tool gradient materials was determined in congruence with the Standard PN-EN ISO 3369:2010. The density of the sinters was measured using the methods of underwater weighing and air weighing. The results were subjected to statistical analysis.

The measurement of open and total porosity was carried out using the following equations:

$$P_o = \frac{m_n - m_s}{m_n - m_w} \times 100\% \quad (2.1)$$

where:

P_o – open porosity [%],

m_s – mass of dry specimen [g],

m_w – mass of underwater weighed specimen [g],

m_n – mass of water saturated specimen [g].

$$P_c = \frac{d - d_p}{d} \times 100\% \quad (2.2)$$

where:

P_c – total porosity [%],

d – true density of the material [g/cm^3],

d_p – apparent density [g/cm^3].

The metallographic tests were carried out on polished sections of the cemented specimens. The specimens were sectioned along the plane perpendicular to the formed layers on the cut-off machine “Minitom” (Struers), using water cooling. Then they were hot mounted in thermohardening resin, ground on diamond shields of the grain size from 220 to 1200 $\mu\text{m}/\text{mm}^2$ at the speed of 300 rev/min and polished on diamond pastes of the granulation from 9 to 1 μm at the velocity of 150 rev/min.

The structure of the fabricated WC-Co tool gradient materials was observed in the scanning electron microscope Supra 35 (Zeiss Company). To obtain the images of the investigated specimens, we applied the detection of secondary electrons (SE) and of backscattered electrons (BSE) with the accelerating voltage from 5 to 20 kV and with the maximum magnification of 20000 times. The quantitative and qualitative X-ray analysis and the analysis of surface distribution of elements was carried out on the ground and polished sections in the scanning electron microscope (SEM) Supra 35 of Zeiss Company furnished with the X-ray energy-dispersive detector EDS.

The texture, grain size and their orientation distribution along the cross-section of WC-Co tool gradient materials was determined using the Electron Backscatter Diffraction method (EBSD) in the scanning electron microscope Supra 35 of Zeiss Company (Fig. 8). Before the testing the specimens were subjected to long-lasting grinding and then polishing with small thrusts using the SiO₂ suspension of the granulation of 0.04 μm. The analysis was carried out with the magnification of 4000x, scanning range of 40 μm x 40 μm, step of 100 nm in four measurement points of the material. In order to improve the image of Kikuchi diffraction lines, the image and background were subjected to averaging. The detachment of background is aimed to eliminate all intensity gradients present on the image and to improve the contrast of diffraction lines, since the algorithms identifying the qualities are more efficient in the case of images having uniform, averaged intensity [29, 40, 44]. The pattern of Kikuchi lines is defining the orientation set-up of each of the investigated microareas dependent on the crystallographic orientation. The diffractions were solved using a program with the application of algorithms allowing for the diversification of Kikuchi lines properties such as width, length, contrast against the surroundings and brightness.

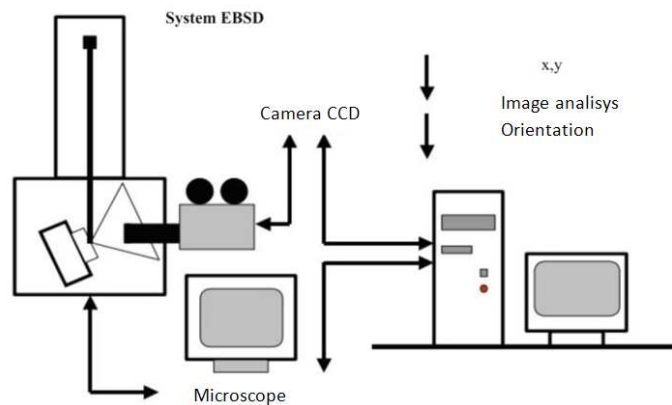


Figure 8. Flow-chart of EBSD system

The analyses of phase composition of cobalt or carbide powders and of cemented gradient materials were carried out with the application of the X-ray diffractometer X'Pert PRO of PANalytical Company in the Bragg-Brentano system, using K α ray filtering of the cobalt tube with the voltage of 40 kV and filament current of 30 mA. The measurement of the secondary radiation intensity was carried out within the angle range 2 Θ from 30 to 120 with the step of

0.05° and calculation time of 10 s using the strip detector Xcelerator in the geometry of grazing incident X-ray diffraction technique with the application of a parallel-beam collimator before the proportional detector.

The diffraction tests and the analyses of the structure of thin foils from the selected places on the specimens from cemented tool gradient materials were carried out in the transmission electron microscope (TEM) JEM 3010UHR of JEOL Company, with the accelerating voltage of 300 kV. Thin foils were prepared from 1mm thick sinters cut off on the MINTOM precision cut-off machine from the cross section of the tool gradient material. The sinters were subjected to semi-mechanical decrement of the thickness of 80 µm on the diamond shield of the gradation of 220 µm/mm², and then to final decrement on an ion polisher using the apparatus of the Gatan Company. The thin foils prepared in this way were investigated in the transmission electron microscope, carrying out the observations in light field and dark field and making the diffraction analyses. The diffractograms from the transmission electron microscope were solved with the Diphra computer program.

The hardness of the materials was determined using the Vickers method with the indenter load of 10 and 300 N respectively. The operating time of the total loading force applied on the indenter was 15 seconds. The measurement was carried out along the whole cross-section width of the cemented specimens, starting the measurement 0.22 mm away from the external surface of the surface layer and finishing the measurement around the base area.

The testing on abrasive wear was carried out with the application of apparatus designed in the Institute of Engineering Materials and Biomaterials of the Silesian University of Technology (Fig. 9). The preparation of specimens for analysis consisted in grinding the surface on a diamond shield of the grain size of 1200 µm/mm² to ensure flat and even surface. On the specimens produced in this way the tests were carried out using a counter-specimen made up by a ceramic ball Al₂O₃ of the diameter of 5.556 mm. The tests were carried out with a diversified number of cycles 1000 and 5000, which translates itself respectively into 4 and 20 m, and with different loading 2.5 and 10 N. Due to the combination of the assumed in this way testing conditions, four results were obtained for the surface layers of each investigated specimen, whereby the abrasive wear could be determined. The same set of tests was carried out for the particular materials of the base, and then the respective measurement results were compared to verify the influence of the structure gradient on the functionality properties. The extent of wear was determined basing on geometric measurement of the wear and calculating its volume. The decrease of volume as the indication of absolute wear is applied when the decay of mass is too small and difficult to estimate [48]. The observation of wear was also

carried out on the confocal microscope LMS 5 Exciter and in the scanning electron microscope (SEM).

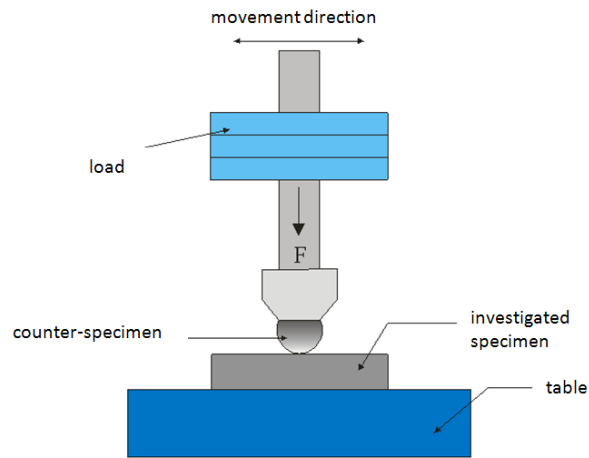


Figure 9. Diagram of the apparatus for testing the resistance to abrasive wear

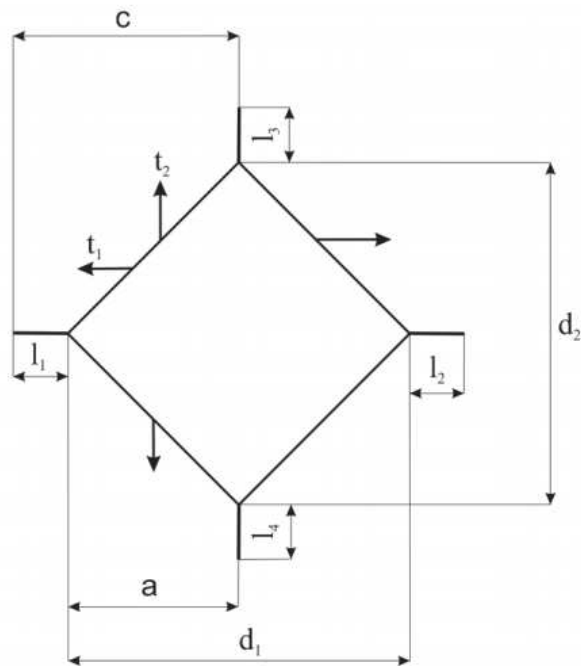


Figure 10. Diagram of the cracking system obtained with Vickers method – Palmqvist method

The tests involving the resistance to brittle cracking (K_{IC}) were performed in congruence with the Standard ISO 28079:2009, making use of the Palmqvist method (Fig. 10). The tests were carried out on the appropriately prepared specimens, polished to eliminate surface stresses which had been introduced to the hard surface layer through the gradation of chemical composition of the material, and then etched in the Murakami reagent of the composition ($[K_3Fe(CN)_6 + KOH + H_2O]$) to ensure a precise read-out of the cracking length.

The following equations were applied to determine the K_{IC} coefficient:

$$H = \frac{1.854 \times P}{[(d_1 + d_2) \times \frac{1}{2}]^2} \quad [N/mm^2] \quad (2.3)$$

where:

P – applied load [N],

d_1, d_2 – length of the imprint diameter [mm].

$$T = l_1 + l_2 + l_3 + l_4 \quad (2.4)$$

where:

T – the total of cracking lengths [mm].

$$K_{IC} = A \sqrt{H} \times \sqrt{\frac{P}{T}} \quad [MNm^{-3/2}] \quad (2.5)$$

where:

A – constant 0.0028.

The results of the investigation studies involving the density, porosity, hardness, abrasive wear and brittle cracking were subjected to statistical workout, calculating for each of the measurement series the arithmetic average, standard deviation and the confidence interval of the average value at the significance level $\alpha = 0.05$. For the measurement results of hardness and brittle cracking of the cemented tool gradient materials, the linear correlation factor was calculated and its significance test was carried out. The said characteristics were determined using the module 'Data analysis' available in Microsoft Excel.

Also the regression function was determined which is approximating the dependence of the

investigated output variable Y (e.g. material hardness or microhardness) on the input variables Xi (e.g. volumetric share of cobalt or temperature).

In the tests on the tool gradient materials of carbide, the finite elements method was applied for the computer simulation of eigen-stresses and strains of material operation [13, 18, 31-35, 53-56]. The true model of the tool gradient material was designed in the program Inventor 11, and the strength analysis was carried out using the program ANSYS 12.0. On account of the predicted simulation range, parametric input files were elaborated which allow to carry out the analysis comprehensively.

In order to carry out the simulation of eigen-stresses of the tool gradient material, the following boundary conditions were accepted:

- the change of cementing temperature is reflected by the cooling process of the specimen from 1400, 1420, 1460°C to the ambient temperature of 22°C,
- for the fabricated material, the material properties were accepted basing on the characteristics cards of MatWeb catalogue which were presented in Table 4.

Table 4. List of mechanical and physical properties accepted in the computer simulation of eigen-stresses occurring in the fabricated material consisting of four layers of a difference share of wolfram carbide and of different cobalt concentration [48, 61]

Properties	Phase composition of the layers of tool gradient material			
	3%Co+97% WC	5%Co+95% WC	7%Co+93% WC	9%Co+91% WC
Young modulus [Pa]10 ⁹	665	640	615	590
Poisson factor	0.2809	0.2815	0.4774	0.5338
Density [kg/m ³]10 ³	15.4	15.1	14.8	14.5
Thermal expansion [1/C] 10 ⁻⁶	4.1	4.3	4.5	4.7
Thermal conductivity [W/ Mc]	98	90	82	76
Specific heat [J/kgC]	138.7	144.5	150.3	156.1
Resistivity (specific resistance) [Ωm]	5.4252	5.442	5.4588	5.4756
Tensile strength [Pa]10 ⁶	1670.75	1641.25	1611.75	1580.25

The model whereof the objective is to determine eigen-stresses of tool operation was worked out using the finite elements method, assuming the true dimensions of the specimen (Fig. 11), where: the first layer – 3%Co+97%WC, the second layer – 5%Co+95%WC, the third layer – 7%Co+93%WC, the fourth layer – 9%Co+91%WC.

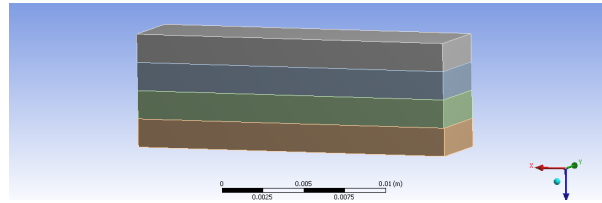


Figure 11. True model of the fabricated material consisting of four layers of different share of wolfram carbide and of different cobalt concentration

The true model was subjected to digitization (Fig. 12). The calculation model consists of 4968 nodes and 760 elements.

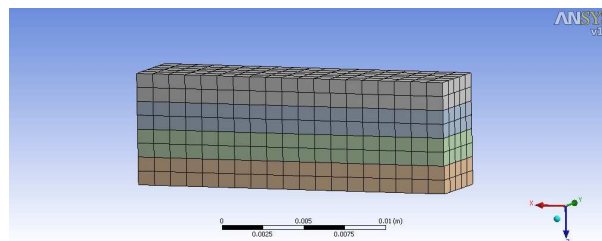


Figure 12. True model of the fabricated material consisting of four layers of different share of wolfram carbide and different cobalt concentration after digitization

For further simulation the same model was applied with the addition of the following boundary conditions:

- the sinter was fixed on one of the sides of the fabricated material by depriving the nodes lying on this plane of all degrees of freedom (Fig. 13),
- the force of 26000 N was applied which was reflecting the operation of the tool (Fig. 13).

The computer simulation was carried out in three stages:

- the first stage involved the simulation of eigen-stresses of the sinter consisting of four layers of different share of wolfram carbide and cobalt depending on the cementing temperature,

- the second stage included the comparative analysis of the computer simulation of the eigen-stresses of the tool gradient material with the experimental results,
- the third stage involved the computer simulation of operation strains of the fabricated tool gradient material applied for example in mining machinery.

The model whereof main objective is to determine eigen-stresses of the fabricated material was made using the finite elements method, assuming the true dimensions of the specimen (Fig. 13).

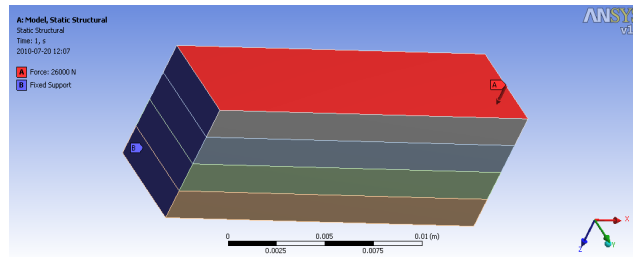


Figure 13. True model of the fabricated material consisting of four layers of different share of wolfram carbide and of different cobalt concentration with the applied boundary conditions

In order to verify the obtained results experimentally through the modeling with the finite elements method on the basis of measurements carried out by means of X-ray spectrometry, the true eigen-stresses in the investigated materials were calculated. The calculations were carried out with the use of $\sin^2\psi$ method, basing on the brand-name program X'Pert Stress Plus. The program has a data base with data indispensable to calculate the values of material constants. Then, the comparative analysis of computer simulation with experimental results was carried out.

3. Results

3.1. Structure, phase and chemical composition of the elaborated gradient materials

Irrespective of the type of cemented materials, their good properties depend on the fabrication and preparation of powders, forming and cementing conditions. In the cementing

process we cannot eliminate potential faults which can be brought about during the preparation of powders or during their formation, and therefore each of the fabrication stages has a considerable influence on the properties of the final product. An appropriate preparation of powder mixtures of homogeneous distribution of WC carbide in cobalt matrix is relevant in view of further pressing and cementing of tool materials. The experimental research demonstrated that the grinding in a high-energy mill yields exceptionally good results as early as after 8 hours. The mixture of powders is forming numerous conglomerates but it is homogeneous, and the cobalt grains surround the WC carbides. The mixture of WC-Co powders after grinding in a ball mill over the same time period is also homogeneous with locally occurring large carbides of the size of about 6 μm which were not fully powdered during the grinding process (Figs. 14, 15).

Irrespective of the applied mill, the rise of grinding time to 20 hours has only slight influence on grain comminution of WC carbide, and hence the grinding time of 8 hours was accepted as optimal.

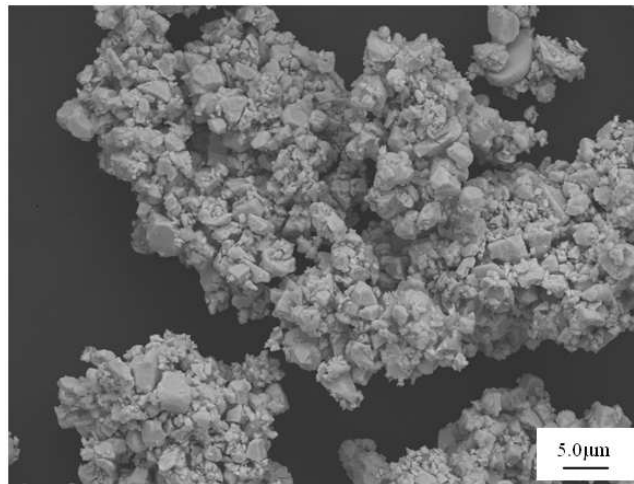


Figure 14. Powder mixture WC (95%), Co (5%) after 8 hours of grinding in a ball mill

For the formation of powders we applied a moulding enabling the pressing of specimens designated to three-point bending after cementing. The prepared powder mixtures of the changing share of WC carbide and appropriate concentration of cobalt matrix were being ground adding paraffin of the 2% volumetric share to reduce the friction between powder

grains and between powder and moulding during the pressing process. Due to small grain size of cobalt and WC carbide, having the average size of maximum 6 μm and connected with it poor flow rate of powder, the formation of further layers of powders mixture of the changing phase share is technologically difficult, and therefore it was agreed that maximum four layers would be formed. Commercial mixtures of WC-Co powders are prepared in the form of granulate of the granulate size of about 0.1 mm, and they are characterized by flow rate of about 30 s. The tests on the flow rate of the produced mixture was not successful since the powders did not pass through the designed for such tests Hall funnel. In spite of poor flow rate and low bulk density of the powders mixture, the compacts were characterized by sharp edges and did not exhibit cracks or chipping. Fig. 16, which presents the compact, illustrates the borders between successive layers. The pressing was carried out within the pressure range applied in the industry from 300 to 450 MPa, and experimentally the pressure for pressing was determined at 340 MPa.

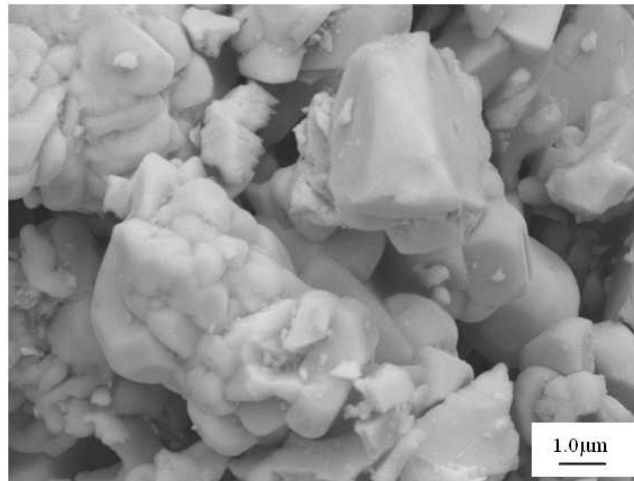


Figure 15. Powder mixture WC (91%), Co(9%)

In order to consolidate the powders we applied unbound sintering, sintering with isostatic condensation or hot isostatic pressing. For the unbound sintering and for the sintering with isostatic condensation we applied the temperature of 1400, 1430 and 1460°C. The hot isostatic sintering was carried out at the temperature of 1420°C.

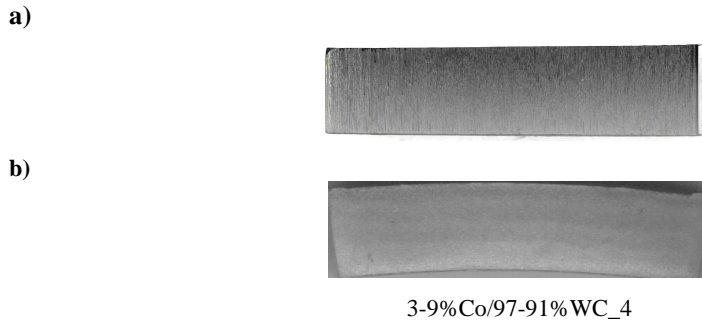


Figure 16. a) Compact pressed under the pressure of 340 MPa, b) sintered tool material

The sintering methods were selected basing on the results described in works [12,20-23, 28,30,43,60] in which, very frequently, for economical reasons or to simplify or accelerate the technological process of the fabricated tool materials, pressing and sintering is combined into one operation. It involves pressing in raised temperature or sintering under pressure. The material obtained in this way is not much porous and its physical and strength properties are considerably better as compared to separate operations of pressing and sintering [18-20,28,35,52,61]. Irrespective of the phase composition of the specimens it can be observed that all materials were deformed after sintering. Undoubtedly, one of the reasons of this deformation is non-homogeneous density of the compact. Numerous pores in lower layers of the compact get condensed during the sintering and hence there is a great contraction in this area. We can observe that the deformation of the specimen in which the phase share of WC powder is changing from 97% in the external layer to 85% in the layer around the core is higher (Fig. 17) as compared to the specimen in which the phase share of WC is changing from 97 to 91% (Fig. 16).

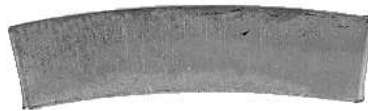


Figure 17. Sintered tool material 3-5%Co/97-85%WC_5

Therefore, in the further studies, we were using specimens in which the share of WC carbide was changing from 97% in the external layer to 91% in the layer around the core. The

appropriateness of the phase composition selected in this way has been confirmed by the research results involving the tests on hardness, density and porosity. Basing on the measurements of density and porosity of the sinters, it was demonstrated that the sintered tool gradient materials based on the powders of wolfram carbide and cobalt are characterized by higher density and lower porosity after sintering with isostatic condensation as compared to the materials after unbound sintering. Analyzing the influence of technological conditions of sintering on density and porosity, it has been demonstrated that the rise of density with the simultaneous decrease of porosity is dependent on temperature, time and technological conditions of sintering (Table 3).

Figures 18-19 present X-ray diffractograms from the investigated tool gradient materials of WC-Co type. The research studies confirmed the presence of phases corresponding to each material type. The X-ray diffractogram contains the reflexes from WC phases and reflexes from Co of the hexagonal structure.

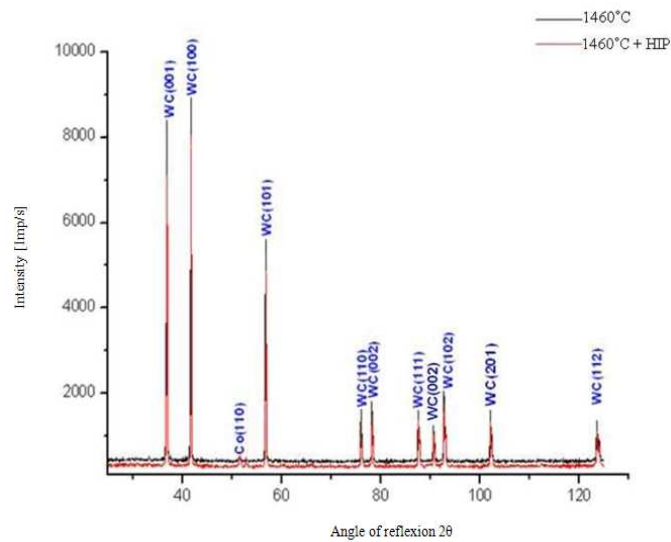


Figure 18. Results of X-ray qualitative phase analysis of tool gradient materials 3-9%Co/97-91WC_4, sintered in a vacuum furnace at temperature $T_{sp}=1460^{\circ}\text{C}$ and subjected to isostatic condensation at $T_{sp}=1425^{\circ}\text{C}$

Basing on the density measurements of the sinters of the newly elaborated tool gradient materials with cobalt matrix, it was found that the highest density is exhibited by the sintered

material with the use of hot isostatic condensation and sintering under pressure. The density of materials obtained in effect of sintering with the use of hot isostatic condensation at the temperature of 1460, 1430 and 1400°C is respectively 14.60, 14.19, 14.16 g/cm³, and the density of materials subjected to unbound sintering at the temperature of 1460, 1430 and 1400°C is respectively 12.96, 13.79 and 14.42 g/cm³. Analyzing the influence of technological parameters of sintering on density, it was found that the density is increasing with a simultaneous decrease of porosity with the rise of time and temperature of the process.

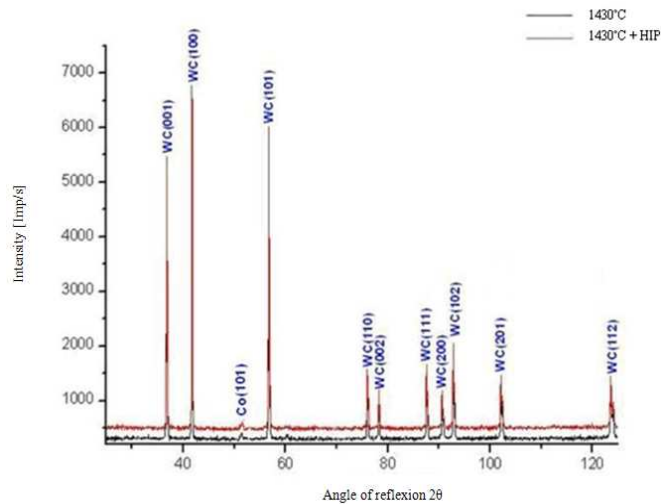


Figure 19. Results of X-ray qualitative phase analysis of tool gradient materials 3-9%Co/97-91WC₄, sintered in the vacuum furnace at temperature $T_{sp}=1430^{\circ}\text{C}$ and isostatically condensed at $T_{sp}=1425^{\circ}\text{C}$

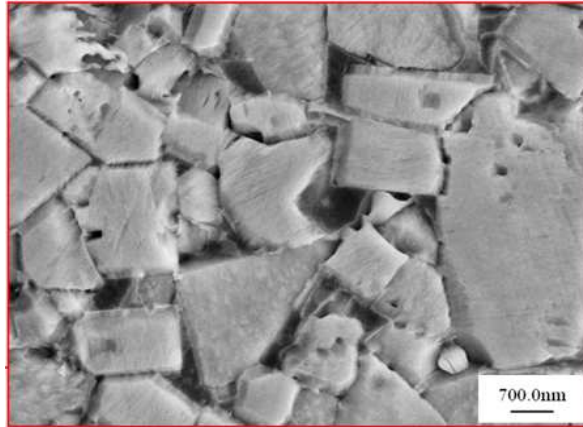
The presence of cobalt in the material results in the formation of liquid phase which during the sintering brings about the formation of low-melting eutectic phase. In this process it is most difficult to maintain the gradient which has a tendency to fade due to the oriented mass transport. In order to avoid such a phenomenon, a high-temperature synthesis with short sintering time is applied [4,15,19,20,53,55,61].

Since most of the infusible grains in the material have the size from 2.5 to 3 micrometers and the dissolution process involves only a small portion of their volume, therefore the final product consists of great oval grains of the basic phase bound by the unified liquid phase (Fig. 20).

In spite of low volumetric share of cobalt, at high sintering temperature this phase is

melting and is partially dissolving the surface of WC carbides. Hence the rise of the volumetric share of liquid phase i.e. low-melting eutectics during the sintering process, which moistens the WC solid phase (Fig. 20). In effect of the above, the capillary forces occurring around grain borders decrease the volume of the pore, increasing in this way the density of the material. The liquid phase during cooling and crystallization assumes the form of small layers separating solid grains (Fig. 20).

a)



b)

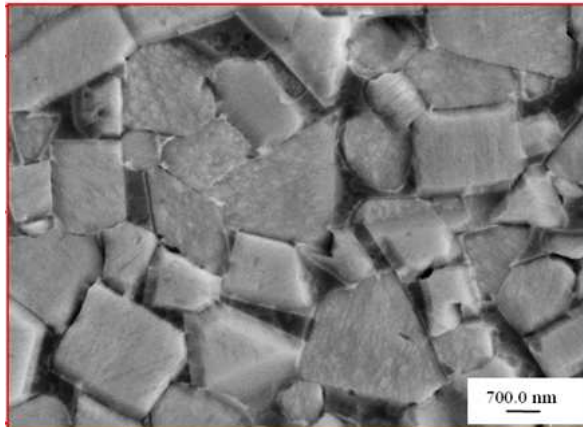


Figure 20. Layer structure a) surface layer b) bottom layer of gradient the material 3-9%Co/97-91%WC_4 sintered in a vacuum furnace at temperature $T_{sp}=1430^{\circ}\text{C}$ and subjected to hot isostatic condensation at the temperature $T_{sp}=1425^{\circ}\text{C}$

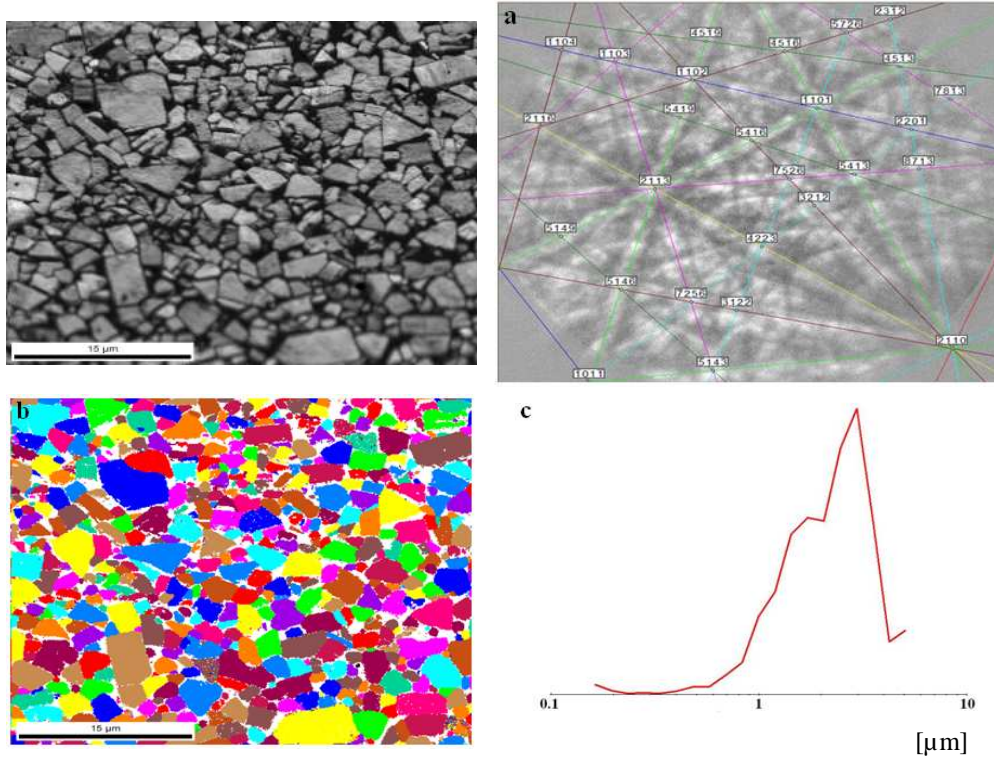


Figure 21. Structure of gradient material 3-9%Co/97-91%WC₄, sintered in the vacuum furnace at temp. $T_{sp}=1400^{\circ}\text{C}$ and subjected to hot isostatic condensation at temp. $T_{sp}=1425^{\circ}\text{C}$, the first layer: a) indexation of the diffraction of the Kikuchi line, b) map of grain size distribution, c) diagram of grain size distribution

The research studies carried out with the use of EBSD method confirmed that the newly elaborated gradient material consists of basic grains of the components of WC and Co powders in which, along the interphase border, there are no microcracks or other discontinuities (Fig. 21). The colored topography maps present the crystallographic orientation of the grains of WC sintered carbides where the particular coloring of the WC grains denotes the normal direction to the surface plane of each grain. The measurements of grain size show that the average size of the grain ranges from 2.5 to 3 μm (Fig. 21c). A considerable decrease of grain size as compared to the input material (6 μm) is connected with the long-lasting milling of the powders of wolfram carbide.

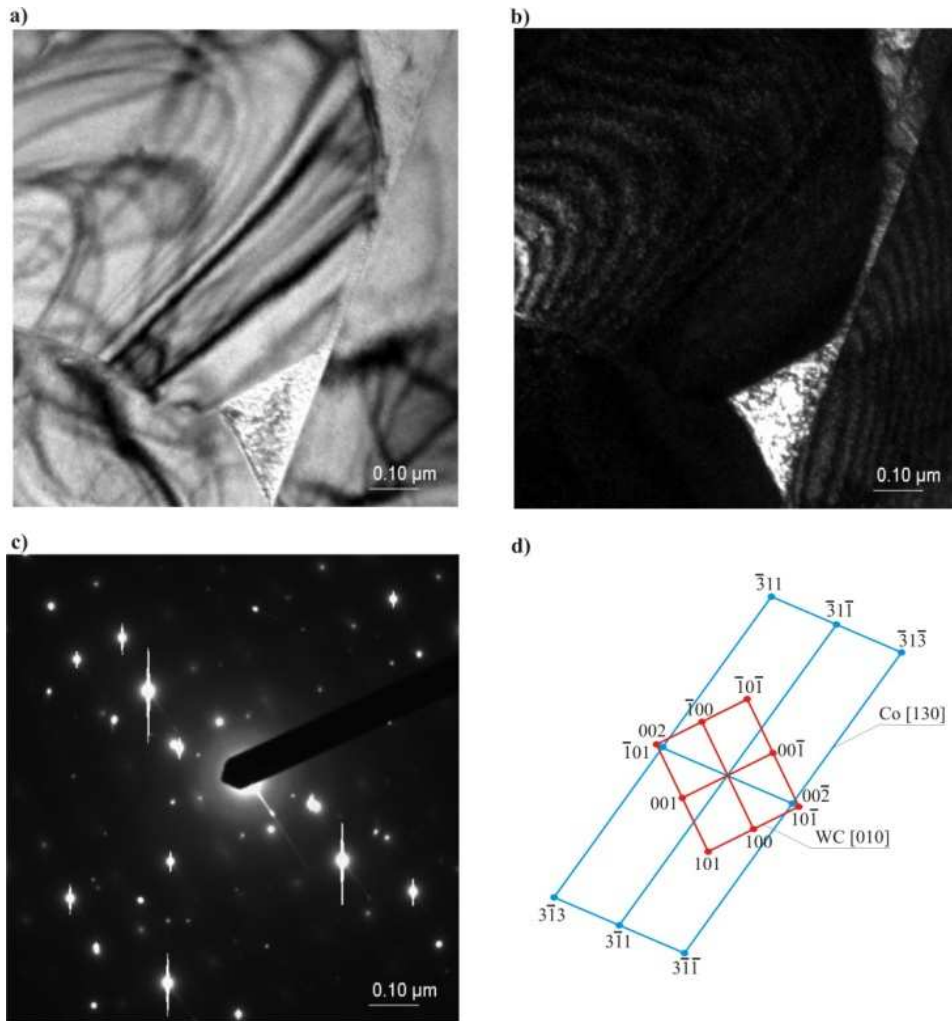


Figure 22. Thin foil structure from WC-Co sintered carbide after sintering at temp. 1460°C; a) image in light field, b) image in dark field from the reflexes (002)Co and (101)WC, c) diffractogram from the area as in Fig. a, d) solution of the diffractogram from the Figure c

The method of X-ray quantitative analysis carried out with the use of X-ray energy-dispersive spectrometer EDS confirms the occurrence of the element W, C and Co respectively in the solid phase of wolfram carbide and in the binding phase of cobalt in the particular layers of the tool gradient material. The newly elaborated tool gradient material is characterized by compact structure due to the uniformly distributed share of binding phase between the solid

phase of carbide. It was also found that the preparation time of mixtures is sufficient enough to ensure that the wolfram carbide grains are coated with cobalt matrix.

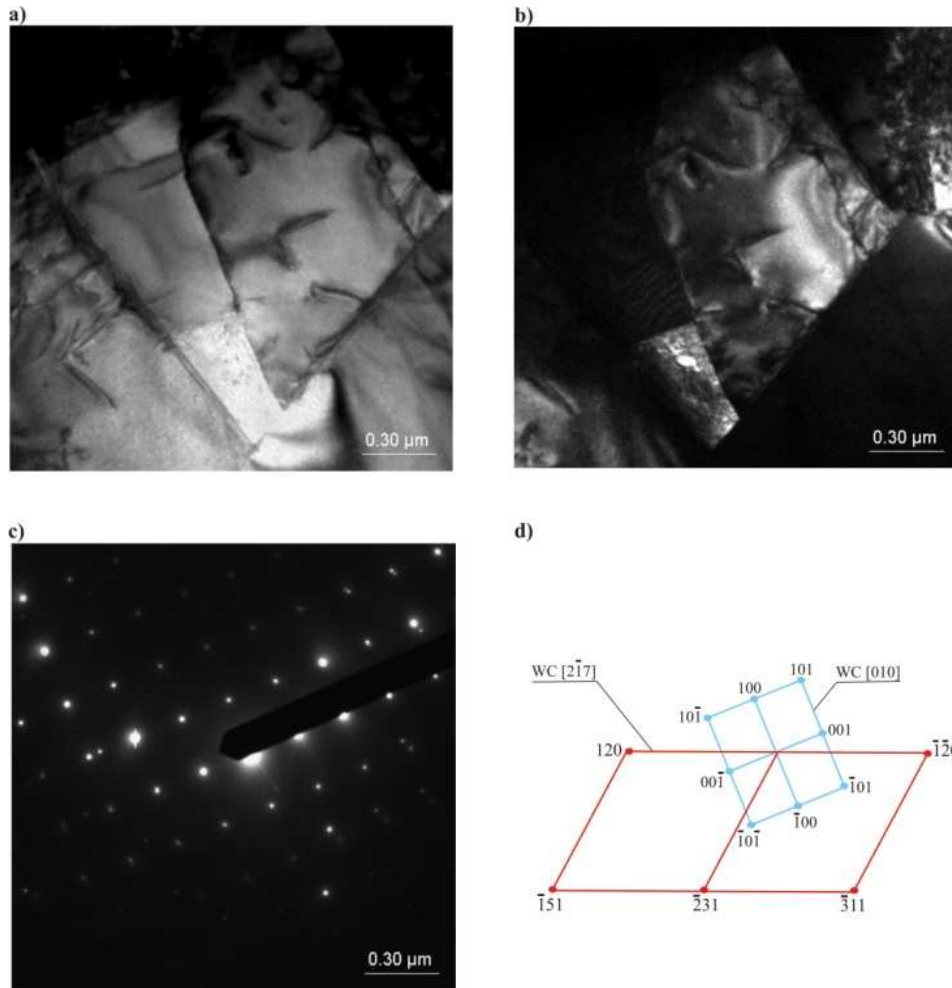


Figure 23. Thin foil structure from WC-Co sintered carbide after sintering at temp. 1460°C; a) image in light field, b) image in dark field from the WC reflexes, c) diffractogram from the area as in Fig. a, d) solution of the diffractogram from Fig. c

In effect of the research on thin foils fabricated in the transmission electron microscope (Figs. 22-24), it was confirmed that the sintered tool gradient materials contain the grains of wolfram carbide and cobalt of the hexagonal network (in the JCPDS file respectively no. 25-

the powder, in effect of which crumbling and fracture of WC grains is taking place. In some WC grains there are subgrains whose disorientation angle is from several to around a dozen degrees. After the sintering process at the temperature of 1400°C we found that in many WC carbide grains there are thin sinters, most probably twins, of the thickness from several to several dozen nm. These sinters are parallel to the WC planes {010} and {110} – as in the four-index Miller-Bravais denotation.

3.2. Mechanical properties and resistance to abrasive wear of the elaborated gradient materials.

The measurement results involving HV hardness (Figs. 26-28) of the fabricated tool materials of the growing share of WC carbide with respect to cobalt matrix in the direction towards tool surface are indicative of a gradual rise of hardness. The hardness of the 3-9%Co/97-91WC_4 material sintered in vacuum, depending on the sintering temperature, can be placed within the range of 1390-1460 HV in the surface layer and is decreasing, with the rise of the distance between the measurement point and the external surface of the surface layer, to 1290-1330 HV in the base (Fig. 26).

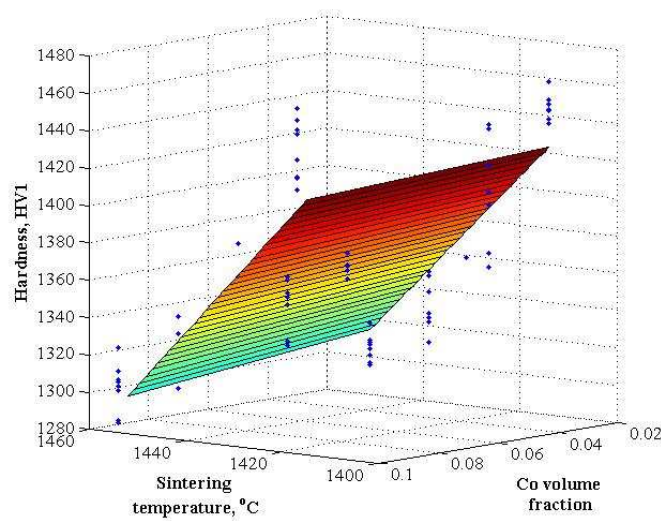


Figure 26. Diagram of regression function describing the relation of HV1 hardness, volumetric share and sintering temperature for the material 3-9%Co/97-91%WC_4

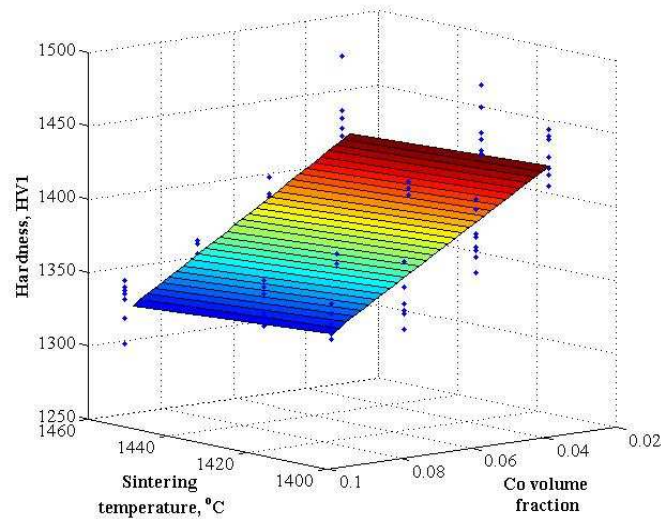


Figure 27. Diagram of regression function describing the dependence of hardness on the volumetric share of cobalt and sintering temperature, for the 3-9%Co/97-91%WC₄ material subjected to sintering and hot isostatic condensation at the temperature of 1425°C in a vacuum furnace

The hardness of the 3-9%Co/97-91WC₄ material sintered and subjected to isostatic condensation at the temperature of 1425°C is within the range of 1430-1470 HV in the surface layer and is decreasing to 1300-1360 HV in the base (Fig. 28). The hardness of the 3-9%Co/97-91WC₄ material sintered with isostatic condensation at the temperature of 1420°C is within the range of 1340-1400 HV in the surface layer and is decreasing, with the rise of the distance between the measurement point and the external surface of the surface layer, to 1310 HV in the base (Fig. 27). In effect of the carried out hardness tests we did not find any considerable difference in hardness of the investigated materials subjected to unbound sintering and those with isostatic condensation.

The relation involving the changes of HV hardness of materials with the changing share of Co phase, volumetric share and sintering conditions was described with the use of a regression function. The value of the multidimensional correlation factor and that of its significance level confirm the correct dependence of hardness on sintering conditions and on cobalt present in particular layers of the material.

Figures 26-28 present the diagrams of regression functions describing the dependence of

hardness on the volumetric share and sintering temperature (T_{sp}) and on the function in the planes defined by the values of input variables, together with confidence intervals at the significance level of $\alpha=0.05$. The carried out measurements demonstrated the influence of sintering technological conditions and volumetric share of WC-Co phases on the hardness of the sintered tool gradient materials.

The research results involving the resistance to brittle cracking K_{IC} of the sintered tool gradient materials of different volumetric share of WC and Co phases in each material layer are presented in Figs. 29-30. The results involving the K_{IC} factor are indicative of a considerable dependence between sintering parameters and the resistance to cracking of particular tool materials. The material 3-9%Co/97-91%WC_4 sintered at the temperature of 1460°C (Figs. 31-35) and the material sintered under pressure at the temperature of 1420°C is characterized by high resistance to brittle cracking. The average value of K_{IC} factor of the surface layer of the material is 15 [$MNm^{-3/2}$] and of the base 18 [$MNm^{-3/2}$].

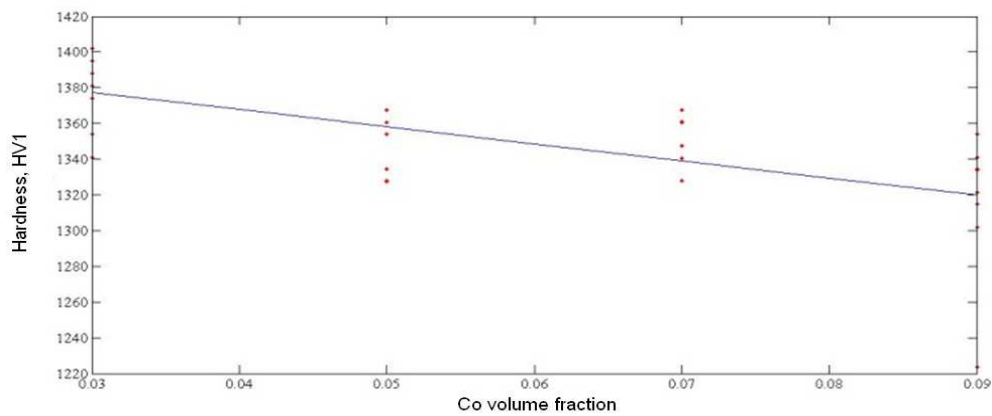


Figure 28. Diagram of regression function describing the dependence of hardness on the volumetric share of cobalt for the 3-9%Co/97-91%WC_4 material subjected to sintering with hot isostatic condensation at the temperature $T_{sp}=1420^{\circ}C$

The average values of the K_{IC} factor of the material sintered at the temperature of 1420°C are respectively 17 [$MNm^{-3/2}$] for the surface layer and 19 [$MNm^{-3/2}$] for the base. The dependence of K_{IC} factor for the investigated materials of different Co concentration on the volumetric share and sintering conditions is presented by means of a regressive function. The value of multidimensional correlation factor and that of its significance level confirm the

dependence of K_{IC} factor on sintering conditions and volumetric concentration of cobalt in the particular layers of the material. Figs. 29-30 present the diagrams of regression functions describing the dependence of K_{IC} factor of the materials on the volumetric share, sintering temperature (T_{sp}) as well as their sections in the planes defined by the selected values of input variables, together with confidence intervals at the significance level of $\alpha=0.05$.

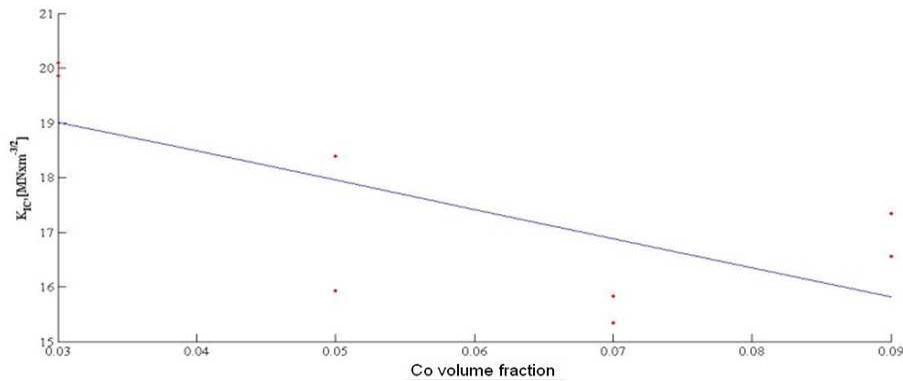


Figure 31. Diagram of the regression function describing the dependence of brittle cracking on the volumetric share of cobalt for the 3-9%Co/97-91%WC_4 material sintered under the pressure in a vacuum furnace at the temperature $T_{sp}=1420^{\circ}\text{C}$

The lack of distinguished difference of the K_{IC} factor in the surface layer and in the base of materials sintered with isostatic condensation can be explained by too long sintering time, resulting in partial or total decay of gradient structure.

The carried out microscopic observations of specimen fractures (Fig. 31) are characterized by hollow systems and convexities, which displays a flaky character of the fracture typical for brittle materials.

The research results involving the resistance of the materials to cracking show that the areas rich in cobalt matrix are characterized by higher K_{IC} factor as compared to the areas rich in WC (Fig. 32).

In order to compare the tribological properties of the fabricated gradient materials, the test on the resistance to abrasive wear was carried out in the system 'investigated specimen and Al_2O_3 ball' as a counter-specimen. The results of the carried out abrasive trial (Table 4) show that the materials sintered with isostatic concentration are characterized by much lower abrasive wear than the materials obtained as a result of unbound sintering. The wear of gradient

materials subjected to unbound sintering, depending on the share of binding phase, temperature, load and number of cycles is presented in Table 4.

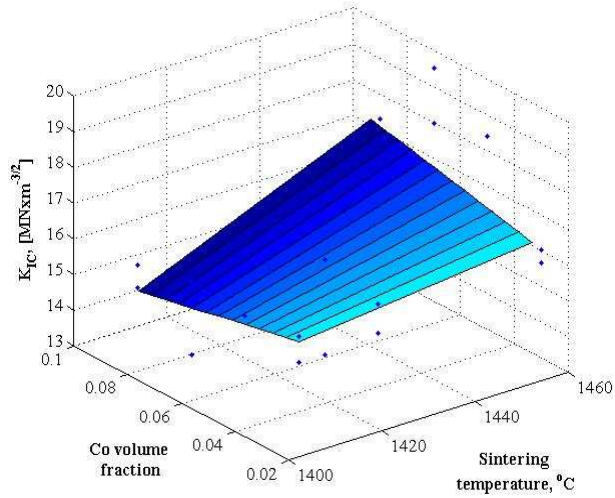


Figure 29. Diagram of the regression function describing the dependence of brittle cracking on temperature and Co volumetric share for the 3-9%Co/97-91%WC₄ material sintered in a vacuum furnace

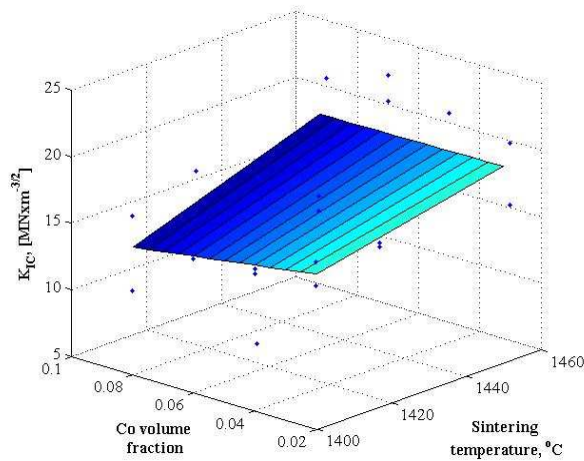


Figure 30. Diagram of the regression function describing the dependence of brittle cracking on temperature, and on cobalt share for the 3-9%Co/97-91%WC₄ material sintered and subjected to hot isostatic condensation at the temperature of 1425°C in a vacuum furnace

The decrement of material is effected by the separation of particles due to micromachining or scratching around the friction areas counter-specimen –material as a result of loose or fixed particles of the abrasive material or sticking out particles of the uneven, hard carbide phase (Fig. 33) [11, 39, 42, 44].

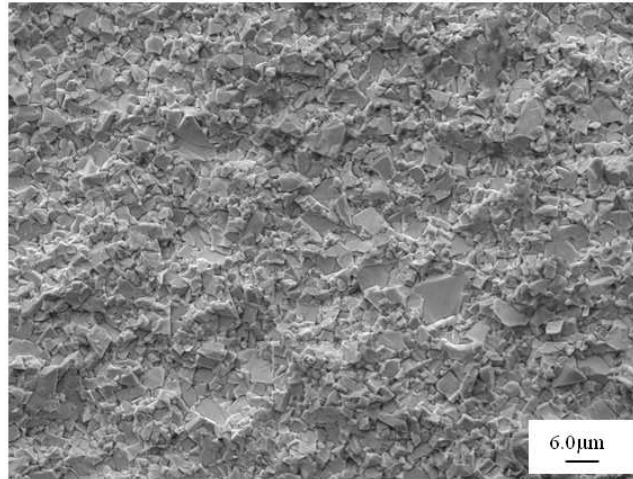


Figure 32. Structure of the fracture of the surface layer of the 3-9%Co/97-91%WC_4 material sintered in a vacuum furnace at the temperature $T_{sp}=1460^{\circ}\text{C}$ and subjected to hot isostatic concentration at the temperature $T_{sp}=1425^{\circ}\text{C}$ in a vacuum furnace

Non-uniform width of the wear bespeaks of the occurrence of wear which consists in sticking of the waste material to the counter specimen which then breaks off in other places causing local unevenness in the place where the wear is lower (Fig. 33). Using the X-ray quantitative microanalysis carried out with the X-ray energy-dispersive spectrometer EDS along the wear path of the material the presence of aluminum and oxygen was confirmed, most probably released by aluminum oxide Al_2O_3 (Fig. 33), due to sticking of waste material to the counter-specimen which then breaks off in other places causing local unevenness around which the wear is lower [9, 10, 17, 30, 44, 51, 55, 56, 58].

The measurement results involving the abrasive wear of the sintered tool gradient materials of wolfram carbide with cobalt matrix are indicative of a gradient change of the properties of the investigated materials, depending on the share of binding phase. Therefore,

the wear of gradient materials is conditioned by many factors: the share of binding phase, loading value of counter-specimen and also the friction path (number of cycles).

3.3. Computer simulation of stresses, strains and displacements of the fabricated gradient material depending on the sintering temperature

Figure 35 presents the results of numerical analysis using the finite elements method gathered in the form of maps of stress distribution in the tool material consisting of four layers of different concentration of wolfram carbide and cobalt for the sintering temperature of 1400, 1420 and 1460°C. The elaborated model of the tool allows to simulate the influence of sintering temperature on stresses (Fig. 35).

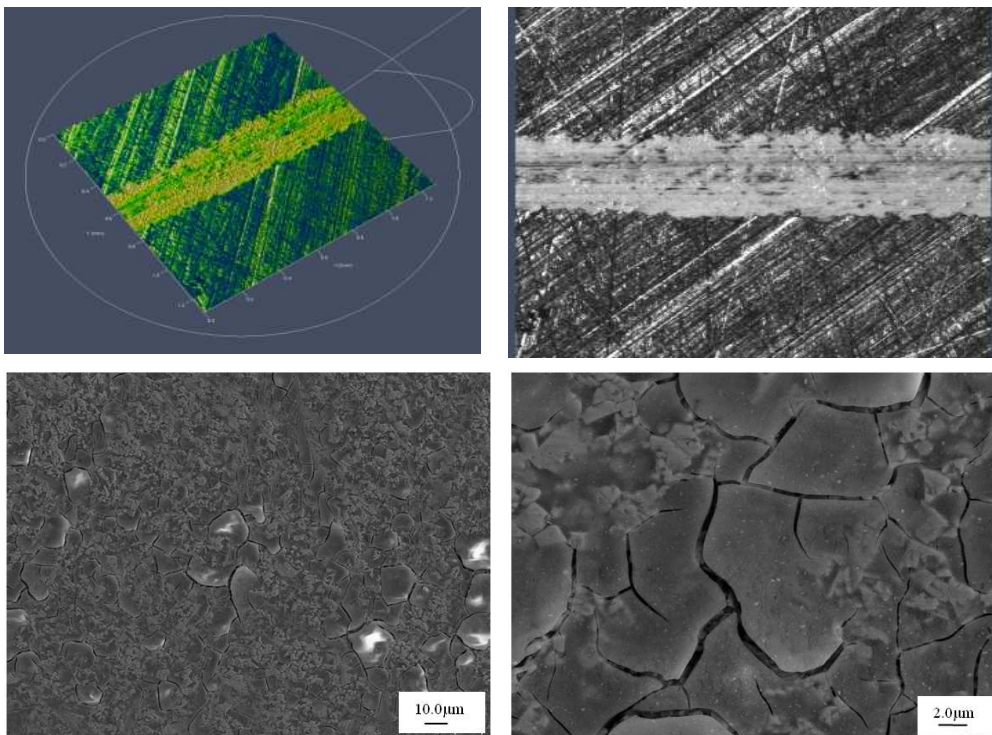


Figure 33. Wear mark of the 3-9%Co/97-91%WC₄ material sintered in vacuum at the temperature of 1400°C and subjected to isostatic condensation at the temperature of 1425°C after 1000 cycles with the load of 10 N in the base

Table 4. Tribological wear of gradient material 3-9%Co/97-91%WC_4

Layer denotation	T_{sp} [°C]	Load [N]	Number of cycles	Statistical quantities	
				Arithmetic average	Standard deviation
97%WC - 3%Co	1460	2.5	5000	4.05×10^{-4}	0.36×10^{-4}
		10	5000	11.63×10^{-4}	0.62×10^{-4}
91%WC - 9%Co		2.5	5000	13.25×10^{-4}	1.22×10^{-4}
		10	5000	23.41×10^{-4}	1.58×10^{-4}
97%WC - 3%Co	1430+1425	2.5	5000	5.43×10^{-4}	0.29×10^{-4}
		10	5000	21.49×10^{-4}	1.71×10^{-4}
91%WC - 9%Co		2.5	5000	6.49×10^{-4}	0.40×10^{-4}
		10	5000	26.60×10^{-4}	2.80×10^{-4}

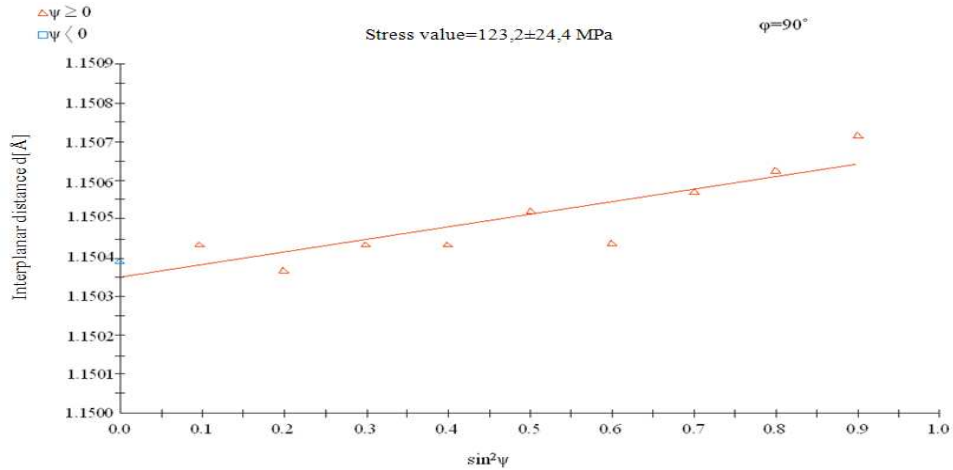


Figure 34. Changes of interplanar distance d of the reflex (201) in the function of $\sin^2\psi$, sintering temperature of 1400°C, 3%Co+97%WC

The calculation results of eigen-stresses in the investigated materials obtained on the basis of reflex shift analysis (201) using the $\sin^2\psi$ method carried out to verify the modeling results are presented in Fig. 34 and in Table 5.

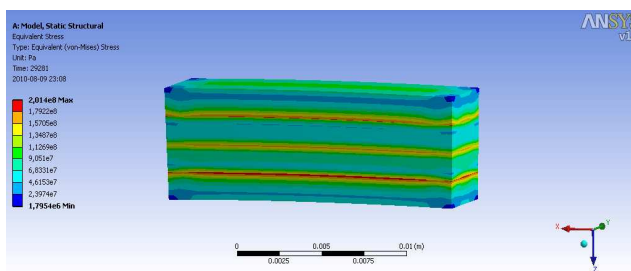


Figure 35. The distribution of simulated eigen-stresses occurring in the cutting edge of a tool consisting of four layers of different share of wolfram carbide and cobalt for the sintering temperature of 1400°C

Basing on the carried out investigation studies it was demonstrated that the highest stress values are characteristic of the material sintered at the temperature of 1460°C. They occur in the surface layer and equal 162 ± 24 MPa, and the simulated stresses equal 170 MPa. The base is characterized by lower stresses as compared to the upper layer. The stresses determined experimentally equal 91 ± 22 MPa and the simulated stresses 80 MPa. The lowest stresses determined experimentally and with the use of computer simulation occur in the tool gradient material sintered at the temperature of 1400°C. The value of these stresses determined experimentally in the upper layer is 123 ± 24 MPa, and the value of simulated stresses equals 116 MPa. The calculated values of stresses in the base are 41 ± 9 and 36 for the simulated stresses.

Table 5. Comparison of stresses obtained experimentally with the results of computer simulation

	Sintering temperature, [°C]	Stresses determined experimentally, [MPa]	Simulated stresses, [MPa]
Upper layer 3%Co+97% WC	1400	123 ± 24	116
	1420	141 ± 7	140
	1460	162 ± 24	170
Bottom layer 9%Co+91% WC	1400	41 ± 9	36
	1420	87 ± 10	80
	1460	91 ± 22	80

The results of eigen-stresses obtained with the computer simulation using the finite elements method are in agreement with the results of stress measurements obtained with the use of $\sin^2\psi$ method (Table 5).

Figures 36-38 present the results of the computer simulation of the fabricated material, allowing for the mechanical loads simulating operating conditions (in mining or drilling machines), gathered as the maps of shifts, strains and stresses distribution.

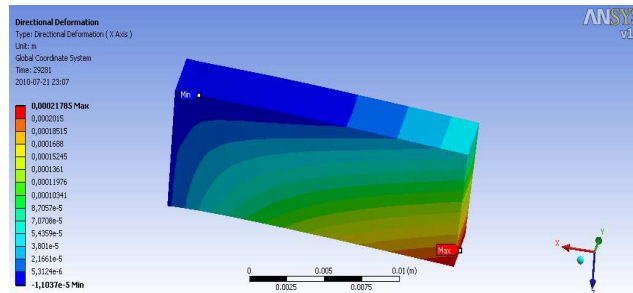


Figure 36. Distribution of the simulated shifts occurring in the cutting edge of a tool consisting of four layers of different share of wolfram carbide and cobalt for the sintering temperature $T_{sp}=1400^{\circ}\text{C}$

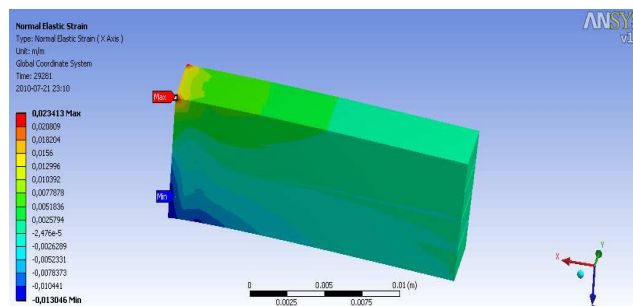


Figure 37. Distribution of the simulated strains occurring in the cutting edge of a tool consisting of four layers of different share of wolfram carbide and cobalt for the sintering temperature $T_{sp}=1400^{\circ}\text{C}$

It was demonstrated, basing on the elaborated model, that through appropriately applied technological procedures, it is possible to evoke tensile stresses in the surface layer of the material, which will increase the resistance of this material to the formation and propagation of

cracks. The difference in the value of heat expansion coefficient in the material is introducing tensile eigen-stresses on the surface of the material after its cooling from the sintering temperature to the ambient temperature.

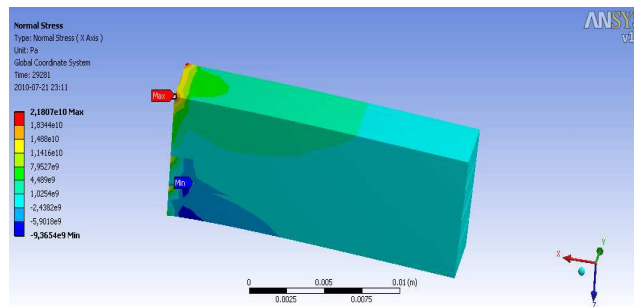


Figure 38. Distribution of the simulated stresses occurring in the cutting edge of a tool consisting of four layers of different share of wolfram carbide and cobalt for the sintering temperature $T_{sp}=1400^{\circ}\text{C}$

Basing on the analysis of the obtained results: among others such as hardness, brittle cracking and abrasive wear it has been demonstrated that this novel method makes it possible to fabricate tool gradient materials resistant to abrasive wear with high resistance to brittle cracking.

4. Conclusions

Basing on the analysis of the obtained results involving sintered tool gradient WC-Co materials, the following conclusions have been formulated:

1. In effect of the carried out investigation studies on the newly elaborated gradient WC-Co tool materials fabricated with a novel technology consisting in sequential coating of the moulding with the layers of WC-Co powder mixtures of the decreasing share of WC carbides from 97 to 91% in the direction from the surface to the core and then pressing and sintering the compacts, the thesis put forward in the PhD dissertation has been proved, and it has been demonstrated that the application of the elaborated fabrication method for the production of tool materials is fully grounded, due to combining non-complementary properties of these materials i.e. resistance to abrasive wear and brittle cracking, due to

gradient structure of the fabricated material which is changing in the continuous way and which is characterized by the rise of the share of hard carbide phase in the direction from the core to the sinter surface and rising share of cobalt matrix concentration in the opposite direction.

2. The applied fabrication method of sintered tool gradient materials necessitates the preparation of WC-Co powder mixtures through their long-lasting milling during which hard and brittle WC carbides of the average equivalent diameter of the grain of $6\ \mu\text{m}$ undergo fragmentation in effect of which their size after sintering does not exceed $3\ \mu\text{m}$, which has a positive influence on the resistance rise to brittle cracking in the sintered state of the fabricated tool materials to $19\ \text{MNm}^{-3/2}$ as compared to $15\ \text{MN}^{-3/2}$ characteristic of the sintered WC-Co materials containing 3% Co produced without gradient.
3. In effect of diffusion processes running during the sintering process, local unification of phase composition in the joint areas is taking place despite the laminar output structure of the compacts fabricated by coating the moulding with successive powder mixtures of a step-wise changing share of WC and Co concentration and then pressing, the gradient of changes of the final structure of the sinter is continuous and not step-wise as in the compact, yet too long heating over 90 min at high sintering temperature of 1460°C , in particular during hot isostatic sintering, results in a decay of gradient structure of the sinter due to the unification of the phase composition within the whole volume of the sinter.
4. Hardness, resistance to abrasive wear and brittle cracking of the sintered tool gradient materials are dependent respectively on the WC share and Co concentration as a binding phase and on the conditions of technological process applied for the fabrication of these materials, i.e. milling of powder mixtures, formation of the compact and sintering, yet the surface of the material is characterized by high hardness of 1460 HV, due to high WC share of 97%, and the core is characterized by higher resistance to brittle cracking $19\ \text{MNm}^{-3/2}$ as compared to the surface because of higher Co concentration of 9%, with the difference of $4\ \text{MNm}^{-3/2}$ between the K_{IC} values on the surface $15\ \text{MNm}^{-3/2}$ and in the core $19\ \text{MNm}^{-3/2}$.
5. Through the application of finite elements method we can model eigen-stresses generated in the newly elaborated tool gradient materials in effect of sintering, having the influence on the properties of these materials, and because the stress values determined through computer simulation are close to those determined experimentally, it is well-founded to apply calculation methods to estimate stresses and to draw conclusions about the trends involving the changes of the properties of the investigated tool gradient material, which necessitates further research.

Acknowledgements

The paper has been realised in relation to the project POIG.01.01.01-00-023/08 entitled “Foresight of surface properties formation leading technologies of engineering materials and biomaterials” FORSURF, co-founded by the European Union from financial resources of European Regional Development Found and headed by Prof. L.A. Dobrzański.



References

1. H.O. Andrén, Microstructure development during sintering and heat-treatment of cemented carbides and cermets, *Materials Chemistry and Physics* 67 (2001) 209-213.
2. Z.G. Ban, L.L. Shaw, Synthesis and processing of nanostructured WC-Co materials, *Journal of Materials Science* 37 (2002) 3397-3403.
3. U. Baste, S. Jacobson, A new view of the deterioration and wear of WC/Co cemented carbide rock drill buttons, *Wear* 264 (2008) 1129-1141.
4. K. Bonny, P. De Baets, J. Quintelier, J. Vleugels, D. Jiang, O. Van der Biest, B. Lauwers, W. Liu, Surface finishing: Impact on tribological characteristics of WC-Co hardmetals, *International Journal of Refractory Metals and Hard Materials* 43 (2010) 40-54.
5. A. Carpinteri, N. Puno, S. Puzzli, Strength vs. toughness optimization of microstructured composites, *Chaos, Solitons and Fractals* 39/3 (2009) 1210-1223.
6. S.I. Cha, K.H. Lee, H.J. Ryu, S.H. Hong, Analytical modeling to calculate the hardness of ultra-fine WC-Co cemented carbides, *Materials Science and Engineering A* 489 (2008) 234-244.
7. J.R. Cho, Optimum material composition design for thermal stress reduction in FGM lathe bit, *Composites: Part A* 37.
8. L.A. Dobrzański, B. Dołżańska, G. Matula, Influence of carbide (W, Ti)C on the structure and properties of tool gradient materials, *Archives of Materials Science and Engineering* 28/10 (2007) 617-620.
9. L.A. Dobrzański, B. Dołżańska, G. Matula, Influence of hard ceramic particles on structure and properties of TGM, *Journal of Achievements in Materials and Manufacturing* 24/2 (2007) 95-98.
10. L.A. Dobrzański, B. Dołżańska, G. Matula, Structure and properties of gradient cermets reinforcer with the (W, Ti)C carbides, *Вісник* 4/2 (2007) 15-20.
11. L.A. Dobrzański, B. Dołżańska, G. Matula, Structure and properties of tool gradient materials reinforced with the WC carbides, *Journal of Achievements in Materials and Manufacturing Engineering* 28/1 (2008) 35-38.

12. L.A. Dobrzański, K. Gołombek, Structure and properties of the cutting tools made from cemented carbides and cermets with the TiN + mono-, gradient – or multi (Ti,Al,Si)N+TiN nanocrystalline coatings, *Journal of Materials Processing Technology* 164-165 (2005) 805-815.
13. L.A. Dobrzański, J. Hajduczek, A. Kloc-Ptaszna, Effect of sintering parameters on structure of the gradient tool materials, *Journal of Achievements in Materials and Manufacturing Engineering* 36/1 (2009) 33-40.
14. L.A. Dobrzański, A. Kloc, G. Matula, J.M. Contreras, J.M. Torralba, Effect of manufacturing methods on structure and properties of the gradient tool materials with the non-alloy matrix reinforced with the HS6-5-2 type high-speed steel, *Proceedings of the 11th International Scientific Conference on the Contemporary Achievements in Mechanics, Manufacturing and Materials Science CAM3S'2005, Gliwice-Zakopane, 2005*, 223-228.
15. L.A. Dobrzański, A. Kloc, G. Matula, J. Domagała, J.M. Torralba, Effect of carbon concentration on structure and properties of the gradient tool materials, *Journal of Achievements in Materials and Manufacturing Engineering* 17 (2006) 45-48.
16. L.A. Dobrzański, A. Kloc-Ptaszna, G. Matula, J.M. Torralba, Structure and properties of a gradient tool materials manufactured using the conventional powder metallurgy method, *Materials Science Forum* (2009) (in print).
17. L.A. Dobrzański, A. Kloc-Ptaszna, G. Matula, J.M. Torralba, Structure and properties of gradient tool materials with the high-speed steel matrix, *Journal of Achievements in Materials and Manufacturing Engineering* 24/2 (2007) 47-50.
18. L.A. Dobrzański, A. Kloc-Ptaszna, G. Matula, J.M. Torralba, Structure and properties of the gradient tool materials of unalloyed steel matrix reinforced with HS6-5-2 high-speed steel, *Archives of Materials Science and Engineering* 28/4 (2007) 197-202.
19. L.A. Dobrzański, A. Kloc-Ptaszna, G. Matula, J.M. Torralba, Structure and Properties of Gradient Tool Materials with HS6-5-2 High-Speed Steel, *Proceedings of the 7th Asia Pacific Conference on Materials Processing, Singapore, 2006*, 128-133.
20. L.A. Dobrzański, A. Kloc-Ptaszna, G. Matula, Properties of sintered gradient tool WC/HS6-5-2 materials, *Proceedings of the 2th International Conference on Modern Achievements in Science and Education, Netanua, Israel, 2008*, 71-76.
21. L.A. Dobrzański, G. Matula, G. Herranz, A. Várez, B. Levenfeld, J.M. Torralba, Metal injection moulding of HS12-1-5-5 high-speed steel using a PW-HDPE based binder, *Journal of Materials Processing Technology* 175 (2006) 173-178.
22. L.A. Dobrzański, G. Matula, A. Várez, B. Levenfeld, J.M. Torralba, Structure and mechanical properties of HSS HS6-5-2 and HS12-1-5-5-type steel produced by modified powder injection moulding process, *Journal of Materials Processing Technology* 157-158 (2004) 658-668.
23. L.A. Dobrzański, G. Matula, A. Várez, B. Levenfeld, J.M. Torralba, Fabrication methods and heat treatment conditions effect on tribological properties of high speed steels, *Journal of Materials Processing Technology* 157-158 (2004) 324-330.

24. L.A. Dobrzański, A. Śliwa, W. Kwaśny, W. Sitek, The computer simulation of stresses in the Ti+TiC coatings obtained in the PVD process, *Journal of Achievements in Materials and Manufacturing Engineering* 17 (2006) 241-244.
25. L.A. Dobrzański, A. Śliwa, W. Sitek, W. Kwaśny, The computer simulation of critical compressive stresses on the PVD coatings, *International Journal of Computational Materials Science and Surface Engineering* 1/1 (2007) 28-39.
26. L.A. Dobrzański, A. Śliwa, W. Sitek, Finite Element Method application for modeling of PVD coatings properties, *Proceedings of the 5th International Surface Engineering Congress*, Washington, USA, 2006, 26-29.
27. L.A. Dobrzański, A. Śliwa, T. Tański, Numerical simulation model for the determination of hardness for casting the magnesium alloys MgMg₁₆Zn₁, *Archives of Materials Science* 29/3 (2008) 118-124.
28. M.H. Enayati, G.R. Aryanpour, A. Ebnonnasir, Production of nanostructured WC-Co powder by ball milling, *International Journal of Refractory Metals and Hard Materials* 27/1 (2009) 159-163.
29. P. Fan, J. Guo, Z.Z. Fang, P. Prichard, Design of cobalt gradient via controlling carbon content and WC grain size in liquid-phase-sintered WC-Co composite, *International Journal of Refractory Metals and Hard Materials* 27 (2009) 256-260.
30. P. Fan, J. Guo, Z.Z. Fang, P. Prichard, Effects of Liquid-Phase Composition on Its Migration during Liquid-Phase Sintering of Cemented Carbide, *Metallurgical and Materials Transactions A* 40/8 (2009) 1995-2006.
31. Z. Fang, G. Lockwood, A. Griffio, A dual composite of WC-Co, *Metallurgical and Materials Transactions A* 30 (1999) 3231-3238.
32. Z.Z. Fang, Correlation of transverse rupture strength of WC-Co with hardness, *International Journal of Refractory Metals and Hard Materials* 23 (2005) 119-127.
33. Z.Z. Fang, O.O. Eso, Liquid phase sintering of functionally graded WC-Co composites, *Scripta Materialia* 52 (2005) 785-791.
34. J.A.M. Ferreira, M.A. Pina Amaral, F.V. Antunes, J.D.M. Costa, A study on the mechanical behaviour of WC/Co hardmetals, *International Journal of Refractory Metals and Hard Materials* 27/1 (2009) 1-8.
35. R. Frykholm, H.O. Andre, Development of the microstructure during gradient sintering of a cemented carbide, *Materials Chemistry and Physics* 67 (2001) 203-208.
36. R. Frykholm, B. Jansson, H.O. Andrén, Methods for atom probe analysis of microgradients in functionally graded cemented carbides, *Micron* 33 (2002) 639-646.
37. R.M. German, A. Eugene, A. Olevsky, Modeling grain growth dependence on the liquid content in liquid-phase-sintered materials, *Metallurgical and Materials Transactions A* 29 (1998) 3057-3067.
38. V.T. Golovchan, N.V. Litoshenko, The stress-strain behavior of WC-Co hardmetals, *Computational Materials Science* 49/3 (2010) 593-597.

39. H.S. Kim, On the rule of mixtures for the hardness of particle reinforced composites, *Materials Science and Engineering A* 289 (2000) 30-33.
40. H.Ch. Kim, I.J. Shon, J.K. Yoon, J.M. Doh, Consolidation of ultra fine WC and WC-Co hard materials by pulsed current activated sintering and its mechanical properties, *International Journal of Refractory Metals and Hard Materials* 25/1 (2007) 46-52.
41. A. Kloc, L.A. Dobrzański, G. Matula, J.M. Torralba, Effect of manufacturing methods on structure and properties of the gradient tool materials with the non-alloy steel matrix reinforced with the HS6-5-2 type high-speed steel, *Materials Science Forum* 539-543 (2007) 2749-2754.
42. I. Konyashin, S. Hlawatschek, B. Ries, F. Lachmann, A. Sologubenko, T. Weirich, A new approach to fabrication of gradient WC-Co hardmetals, *International Journal of Refractory Metals and Hard Materials* 28/2 (2010) 228-237.
43. M.T. Laugier, Palmqvist toughness in WC-Co composites viewed as a ductile/brittle transition, *Journal of Materials Science Letters* 6 (1987) 768-770.
44. A. Lawley, T.F. Murphy, Metallography of powder metallurgy materials, *Materials Characterization* 51 (2003) 315-327.
45. G.H. Lee, S. Kang, Sintering of nano-sized WC-Co powders produced by a gas reduction-carburization process, *Journal of Alloy and Compounds* 419 (2006) 281-289.
46. W. Lengauer, K. Dreyer, Functionally gradient hardmetals, *Journal of Alloys and Compounds* 338 (2002) 194-212.
47. W. Lengauer, K. Dreyer, Tailoring hardness and toughness gradients in functional gradient hardmetals (FGHMs), *International Journal of Refractory Metals and Hard Materials* 24 (2006) 155-161.
48. K. Liu, X.P. Li, Ductile cutting of tungsten carbide, *Journal of Materials Processing Technology* 113 (2001) 348-354.
49. W. Liu, X. Song, J. Zhang, F. Yin, G. Zhang, A novel route to prepare ultrafine-grained WC-Co cemented carbides, *Journal of Alloys and Compounds* 458/1-2 (2008) 366-371.
50. G. Matula, L.A. Dobrzański, B. Dołżańska, Influence of cobalt portion on structure and properties of FGHM, *International Journal of Materials and Product Technology* 33/3 (2008) 280-290.
51. G. Matula, L.A. Dobrzański, B. Dołżańska, Structure and properties of TGM manufactured on the basis of cobalt, *Journal of Achievements in Materials and Manufacturing* 20 (2007) 151-154.
52. G. Matula, L.A. Dobrzański, G. Herranz, A. Várez, B. Levenfeld, J.M. Torralba, Influence of Binders on the Structure and Properties of High Speed-Steel HS6-5-2 Type Fabricated Using Pressureless Forming and PIM Methods, *Materials Science Forum* 534-536 (2007) 693-696.
53. A. Śliwa, L.A. Dobrzański, W. Kwaśny, W. Sitek, The computer simulation of internal stresses on the PVD coatings, *Archives of Computational Materials Science and Surface Engineering* 1/3 (2009) 183-188.
54. A. Śliwa, W. Kwaśny, L.A. Dobrzański, Computer simulation of stresses in coatings obtained the PVD process, *Engineering Materials* 31/3 (2010) 732-734.

55. G.S. Upadhyaya, *Cemented tungsten carbides, Production, Properties and Testing*, Westwood, New Jersey, U.S.A., 1998.
56. G.S. Upadhyaya, *Materials science of cemented carbides – an overview*, *Materials and Design* 22 (2001) 483-489.
57. X. Wang, Z.Z. Fang, H.Y. Sohn, *Grain growth during the early stage of sintering of nanosized WC-Co powder*, *International Journal of Refractory Metals and Hard Materials* 26 (2008) 232-241.
58. X. Wu, J. Guo, *Electric-discharge compaction of graded WC-Co composites*, *International Journal of Refractory Metals and Hard Materials* 27/1 (2009) 90-94.
59. H. Zhang, Q. Lu, L. Zhang, Z. Zak Fang, *Dependence of microcrack number density on microstructural parameters during plastic deformation of WC-Co composite*, *International Journal of Refractory Metals and Hard Materials* 28 (2010) 434-440.
60. H. Zhang, Z. Zak Fang, Q. Lu, *Characterization of a bilayer WC-Co hardmetal using Hertzian indentation technique*, *International Journal of Refractory Metals and Hard Materials* 27 (2009) 317-322.
61. www.webelements.com